Brain Stimulation 16 (2023) 1062–1071

Contents lists available at ScienceDirect

Brain Stimulation

journal homepage: www.journals.elsevier.com/brain-stimulation

Functional connectivity explains how neuronavigated TMS of posterior temporal subregions differentially affect language processing

Maria Vasileiadi [a], Anna-Lisa Schuler [a], Michael Woletz [a], David Linhardt [a], Christian Windischberger [a], Martin Tik [a,b,*]

[a] Center for Medical Physics and BME, Medical University of Vienna, Vienna, Austria
[b] Department of Psychiatry & Behavioral Sciences, Stanford University, Stanford, CA, USA

ARTICLE INFO

Keywords:
Transcranial magnetic stimulation (TMS)
Language
Functional connectivity
E-field modeling

ABSTRACT

Background: "Wernicke's area" is most often used to describe the posterior superior temporal gyrus (STG) and refers to a region traditionally thought to support language comprehension. However, the posterior STG additionally plays a critical role in language production. The purpose of the current study was to determine to what extent regions within the posterior STG are selectively recruited during language production.

Methods: 23 healthy right-handed participants completed an auditory fMRI localizer task, resting-state fMRI and underwent neuronavigated TMS language mapping. We applied repetitive TMS bursts during a picture naming paradigm to probe speech disruptions of different categories (anomia, speech arrest, semantic paraphasia and phonological paraphasia). We combined an in-house built high precision stimulation software suite with E-field modeling to map the naming errors to cortical regions and revealed a dissociation of language functions within the temporal gyrus. Resting state fMRI was used to explain how E-field peaks of different categories differentially affected language production.

Results: Peaks for phonological and semantic errors were found in the STG while those for anomia and speech arrest were located in the MTG. Seed-based connectivity analysis revealed a local connectivity pattern for phonological and semantic errors, while anomia and speech arrest seeds resulted in a larger network between IFG and posterior MTG.

Conclusions: Our study provides important insights into the functional neuroanatomy of language production and might help to increase the current understanding of specific language production difficulties on a causal level.

1. Introduction

"Wernicke's area" is most often used to describe the posterior superior temporal gyrus (STG)/angular gyrus and refers to a region traditionally thought to support language comprehension [1–3]. While traditionally Broca's area, located in the inferior frontal gyrus (IFG) [4], plays a critical role in language production, modern neuroimaging and lesion studies converge on the conclusion that "Wernicke's area", and the posterior temporal lobe in a broader sense, additionally play a critical role in speech production [4–10]. Further, different subregions of these two larger language areas (i.e. IFG and STG) might be related to distinct functions of language production.

Evidence to support this differentiation is based on direct current stimulation (DCS) and transcranial magnetic stimulation (TMS) studies. These studies are based on qualitative error evaluation during object naming while the participant is getting stimulated. Using DCS [11,12] could show probabilistic evidence for different qualitative errors (i.e. semantic errors, phonological errors, anomia and speech arrest) due to stimulation, to be mapped to the STG and middle temporal gyrus (MTG). Although DCS might be the most focal measure for functional disruption, it is invasive and samples are limited to the brain area where surgery is performed.

There is further evidence for the distribution of these qualitative errors in the posterior temporal lobe based on none-invasive transcranial magnetic stimulation in patients and healthy subjects [13–23]. However, these studies are limited by considering the stimulated target as the area underneath the center of coil or even parcellation as the functional area and show inconclusive mapping results. Importantly, the real stimulation effects of a given coil position are depending on how the magnetic field generated by the coil in a given position interacts with the

* Corresponding author. Lazarettgasse 14, 1090 Vienna, Austria.
E-mail address: martin.tik@meduniwien.ac.at (M. Tik).

https://doi.org/10.1016/j.brs.2023.06.014
Received 31 December 2022; Received in revised form 25 May 2023; Accepted 21 June 2023
Available online 28 June 2023
1935-861X/© 2023 The Author(s). Published by Elsevier Inc. This is an open access article under the CC BY-NC-ND license (http://creativecommons.org/licenses/by-nc-nd/4.0/).

individual's brain architecture (gyrification).

The spatial resolution of causal function to cortex mapping can be advanced by introducing electric field (E-field) modeling. This approach has been successfully used to map hand muscles with high accuracy [24–26]. However, language functions show a more widespread network of remotely connected areas. Therefore, multimodal approaches might be employed to understand functional engagement of cortical areas beyond the primary motor cortex. In this respect, TMS effects have been suggested to not only affect the area directly beneath the coil, but to influence remote and interconnected areas [27–34]. In addition, it has been shown that TMS has different modulatory effects on brain connectivity depending on the cortical target region [35]. More specifically, low frequency TMS stimulation over areas involved in cognitive versus sensory processing show opposing network signaling effects. Resting-state fMRI (rs-fMRI) is a straightforward method to map individuals connectivity patterns and can be combined with offline data in order to compare general connectivity patterns of participants based on regions of interest [36]. The aim of the present study was to differentiate subregions within the posterior temporal lobe based on their selective involvement in language production.While presurgical mapping typically follows established protocols for language mapping with TMS [37], we aimed to investigate and dissociate specific cognitive subfunctions using TMS. By incorporating E-fields, we anticipated potential improvements in our investigation in this respect. To achieve this,we systematically applied multiple short bursts of repetitive TMS (rTMS) to nodes of a target grid centered around a functionally defined language peak (fMRI language localizer) within the STG while subjects performed a picture naming paradigm. We categorized naming errors as anomia (no response), speech arrest (delay/hesitation), semantic paraphasia (e.g., "car" instead of "tractor") and phonological paraphasia (e.g., "ectepus" instead of "octopus") [12]. Combining an in-house built high precision navigation software and E-field modeling, we map naming errors to cortical regions revealing a dissociation of language functions within the temporal gyrus. In order to explain the functional selectivity of the resulting maps, we performed resting-state network analysis for each peak of the E-field derived maps.

2. Material and methods

2.1. Sample

23 healthy right-handed native German speakers (14 female, 9 male, mean age: 27.39, SD: 6.80) participated in this study. All subjects were confirmed to be right-handed based on the Edinburgh Handedness Inventory (mean score: 88.24, SD: 12.45). None of the participants reported any history of neurological or psychiatric disorders and no language deficits. Participants were recruited from the general public and were financially reimbursed for their participation. The study protocol was approved by the ethics board of the Medical University of Vienna and conducted in accordance with the declaration of Helsinki. After a description of the study was provided, all participants gave written informed consent.

2.2. MRI data acquisition and preprocessing

To optimize the delineation of individualized stimulation targets in subjects, we employed fMRI to identify language-associated areas before conducting nTMS language mapping.To achieve this, we administered an auditory description decision task (ADDT [38]). The paradigm consisted of alternating blocks of experimental and baseline conditions. The task consisted of 10 blocks (five of each condition), each block lasting 30 s. Each block consisted of 10 stimuli which were presented every 4 s. In the experimental condition participants were presented with sentences either accurately or inaccurately describing a common, concrete noun embedded in the same syntactic frame (e.g., "What you write with is a pen.", "What you sit on is a window."). Participants indicated the incorrect items via button press. The sentences from the original paradigm as described in Ref. [38] were translated and recorded by a native female German speaker and presented using MRI compatible, passively noise reducing in-ear headphones. In the baseline condition the sentences were played in reverse and some items were followed by a tone. Participants were instructed to indicate the presence of the tone by pressing a button. The baseline items matched the experimental items in required responses, length of utterances and presentation volume. Functional MRI data were acquired on 3T (Siemens PRISMA, 64-channel head-coil) using the CMRR EPI sequence [39] (TR = 1000 ms, TE = 38 ms, flip angle 62°, multiband factor = 4, 40 slices, 500 vol, voxel size = 2.3 x 2.3 × 3 mm^3). In order to assess functional connectivity, we acquired resting-state data with an optimized echo time (TE) [40] (TR = 500 ms, TE = 38 ms, flip angle 60°, multiband factor = 4, 84 slices, 1200 vol, voxel size = 3 mm^3). Participants were instructed to relax, think of nothing in particular and let their mind wander. A fixation cross was presented via a digital projector connected to a computer. The resting-state scan lasted 6 min and 16 s. In addition, a T1-weighted image was acquired for anatomical reference and for E-field modeling (TR = 2100 ms, TE = 3.67 ms, flip angle 8°, voxel size = 1 mm^3 isotropic). The resting-state preprocessing pipeline is described elsewhere [36,39] and the full custom preprocessing pipeline can be found in the Supplementary Materials. In short: resting-state fMRI data were de-spiked (AFNI 3dDespike), slice-time corrected (FSL) [41], bias-field corrected (ANTs) [42], realigned (FSL), spatially normalized to MNI space (ANTs) and spatially smoothed with a 6 mm FWHM Gaussian kernel (FSL) using a custom preprocessing pipeline. Preprocessing of the functional task fMRI data was performed in SPM12. Data were realigned, coregistered, spatially normalized to MNI space and spatially smoothed with a 6 mm FWHM Gaussian kernel. A one-sample *t*-test was performed and single-subject t-maps ($p < 0.05$ FWE corrected) were generated by comparing the forward blocks and backward blocks on a voxel-wise basis with button presses as a regressor of non-interest. The individual non-normalized activation maps resulting from the contrast forward > backward were used as an overlay for the TMS language mapping procedure.

2.3. Experimental setup

A summary of the experimental setup and procedure is provided in Fig. 1. The TMS language mapping was performed using an MRi-B91 MR-compatible TMS coil connected to a Magventure MagProX100 stimulator (Magventure, Farum, Denmark). First, the T1-weighted MRI scan of each participant and the participant's head were co-registered using neuronavigation (Brainsight 3, Rogue research Inc., Canada). Second, for each participant the resting motor threshold (rMT) was defined. The primary motor cortex (M1) target area was identified via neuronavigation including Polaris optical position sensor (Northern Digital, Waterloo, ON, Canada) and the coil was positioned parallel to the skull in a 45° angle in relation to the midline. Single TMS-pulses were applied at an intensity of 70% of the maximum stimulator output. Three EMG-electrodes were placed in a belly-tendon application on the first dorsal interosseus muscle (FDI) of the dominant right hand. After the FDI peak had been defined, the stimulation intensity was decreased until the lowest intensity was found at which 5 out of 10 pulses resulted in a motor evoked potential (MEP) response between 0.05 and 0.1 mV within a time frame between 15 and 35 ms. This rMT was then used as a basic value for the TMS mapping procedure in which we stimulated at 100% of the rMT.

2.4. TMS language mapping procedure

For each participant, the task fMRI results were overlaid onto their respective anatomical scan using the neuronavigation software. The individual language 'peak' within the posterior temporal gyrus was defined as the maximum activation and acts as the center of a circular

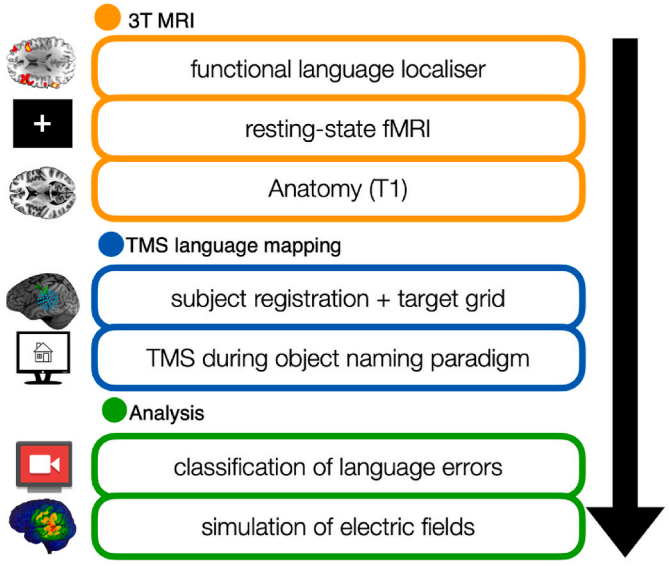


Fig. 1. Summary of experimental setup and procedure. Functional and structural imaging was performed ahead of the TMS language mapping paradigm. The T1w anatomy was loaded into the neuronavigation software for subject registration. The activation from the fMRI localizer task was loaded as an overlay. A target grid was defined around the language peak. The Precision Stimulation Software was used to perform the TMS during an object naming paradigm. Afterwards the recordings of the sessions were analyzed, and language errors were classified. E-fields were simulated for each stimulation target.

TMS target grid. The target grid consisted of 5 rings comprising 40 targets spaced 5 mm from each other. Following the recommendations for posterior language mapping protocols [23], TMS-bursts of 10 Hz (5 biphasic pulses per burst) were applied to each node of the target grid with a coil orientation 90° in relation to the gyrus. Each target node was addressed three times in a randomized order during an object naming task. After correct positioning of the coil (see below), the pictures were displayed for 500 ms and stimulation occurred with a 200 ms delay allowing for visual awareness of the picture [43]. The set of pictures consisted of 60 black and white drawings of common objects presented in randomized order [44]. The minimum delay between subsequent stimulation and the next picture onset was set to 1 s. Prior to the TMS mapping procedure, baseline performance in picture naming was assessed. Pictures that could not be named correctly were omitted from the set of pictures. After recording the participants' baseline, the TMS mapping procedure was started. Participants were instructed to name the objects as quickly as possible and to respond with the first word that comes to their mind in their native language (i.e., German). The procedure was video recorded from two camera angles, one angle optimized to best capture the participants face filmed from the Macintosh PC and a second angle filmed from a smartphone to capture the scene including the presentation screen. To improve audio quality, an omni-directional microphone (BY-M1, Boya, 2018) was clipped onto the participants' clothing 20 cm away from the mouth.

2.5. Precision stimulation software (PSS)

The PSS was developed to deliver TMS pulses with high precision in order to limit variability in responses due to coil misplacement. Different from existing public software, the PSS does not only present the current coil position to the user, but is also actively involved in the triggering process of a TMS pulse. To do so, the operator has to enable the triggering process with a foot pedal, while the software automatically triggers the stimulus presentation as well as the TMS pulse, once the coil position is on target. The PSS combines neuronavigation, control of the TMS device and data acquisition in one single software. The software was running on a Macintosh computer. A screenshot is shown in Fig. 2.

In the current study, the software was used to address all nodes from the previously defined target grid three times in a randomized order and to ensure that stimulation only occurred when the TMS coil was precisely on the target. Specifically, the coil displacement was limited by 2 mm, the tilt by 5°, the rotation by 5° and the coil-to-cortex distance by 5 mm. The previously made neuronavigation project was loaded into the PSS. The software ensured precise timing of stimulation and was also used to present the pictures on the connected monitor. The exact coil positions at time of stimulation were saved for post-hoc simulation of the E-fields for each target.

2.6. TMS data analysis

The video recordings from the Apple Macintosh PC and the smartphone were combined for offline assessment with an in-house written software utilizing moviepy (https://zulko.github.io/moviepy/). The software synchronizes both videos to the TMS stimulation and annotates each stimulation event with the corresponding meta-data for ease of analysis. An example frame from the combined video is shown in Fig. 3.

The detected language errors were documented and categorized into four groups: anomia (no response), speech arrest (delay/hesitation), semantic paraphasia (e.g., "car" instead of "tractor") and phonological paraphasia (e.g., "ectepus" instead of "octopus") [12]. Language errors seemingly related to muscle stimulations or pain were excluded from the analysis. Two independent raters with ample experience in language research analyzed all videos (authors M.V. and A.L.S.). The raters were blinded to the location of the stimulation sites to ensure objective evaluation. If raters' scores did not correspond, a third rater (author M. T.) evaluated the item and resolved the discrepancy. After the video analysis, the electric fields for the coil positions leading to the detected language errors were simulated in subject space using SimNIBS (SimNIBS 3.2.6 [45]) using a MRI-B91 (Magventure) coil model [46]. The SimNIBS pipeline basically involves three steps: 1) automatic segmentation of MRI images and meshing to create individualized head models, 2) E-field calculation using the Finite Element Method (FEM), and 3) post-processing of results for further analysis. All E-field analyses were performed in MNI space. We used the *subject2mni* function from SimNIBS to spatially normalize the electric fields to MNI space to allow for group level analysis. For the second level analysis, we merged the spatially normalized electric fields for each language error type and then averaged them, resulting in four mean E-field maps, i.e. one for each error type.

2.7. Resting-state fMRI analysis

All statistical analyses of resting-state fMRI were performed in MNI space. For single-subject (first level) analysis, the mean E-field was calculated for each language error category independently. The peaks within the individuals mean E-field maps for each language error category were extracted. The MNI coordinates of the extracted peaks served as the center for spherical ROIs that were created with a radius of 6 mm. Seed-voxel correlations were calculated for each ROI, resulting in resting-state networks per language error category (i.e., anomia, speech arrest, semantic paraphasia and phonological paraphasia). The resulting resting-state network connectivity maps were used for group analysis. A flexible factorial design (as implemented in SPM12) was computed representing one factor (naming error) with four conditions (anomia, speech arrest, semantic paraphasia and phonological paraphasia). Linear regression was performed at each voxel, using generalized least squares with a global approximate AR(1) autocorrelation model, drift fit with Discrete Cosine Transform basis (128 s cutoff). Contrasts were calculated for each of the four naming error categories as well as the contrasts between each respective naming error category. Threshold of the t-statistics was set to $p < 0.05$ and cluster-wise FWE correction was performed (initial cluster defining threshold $p < 0.001$).

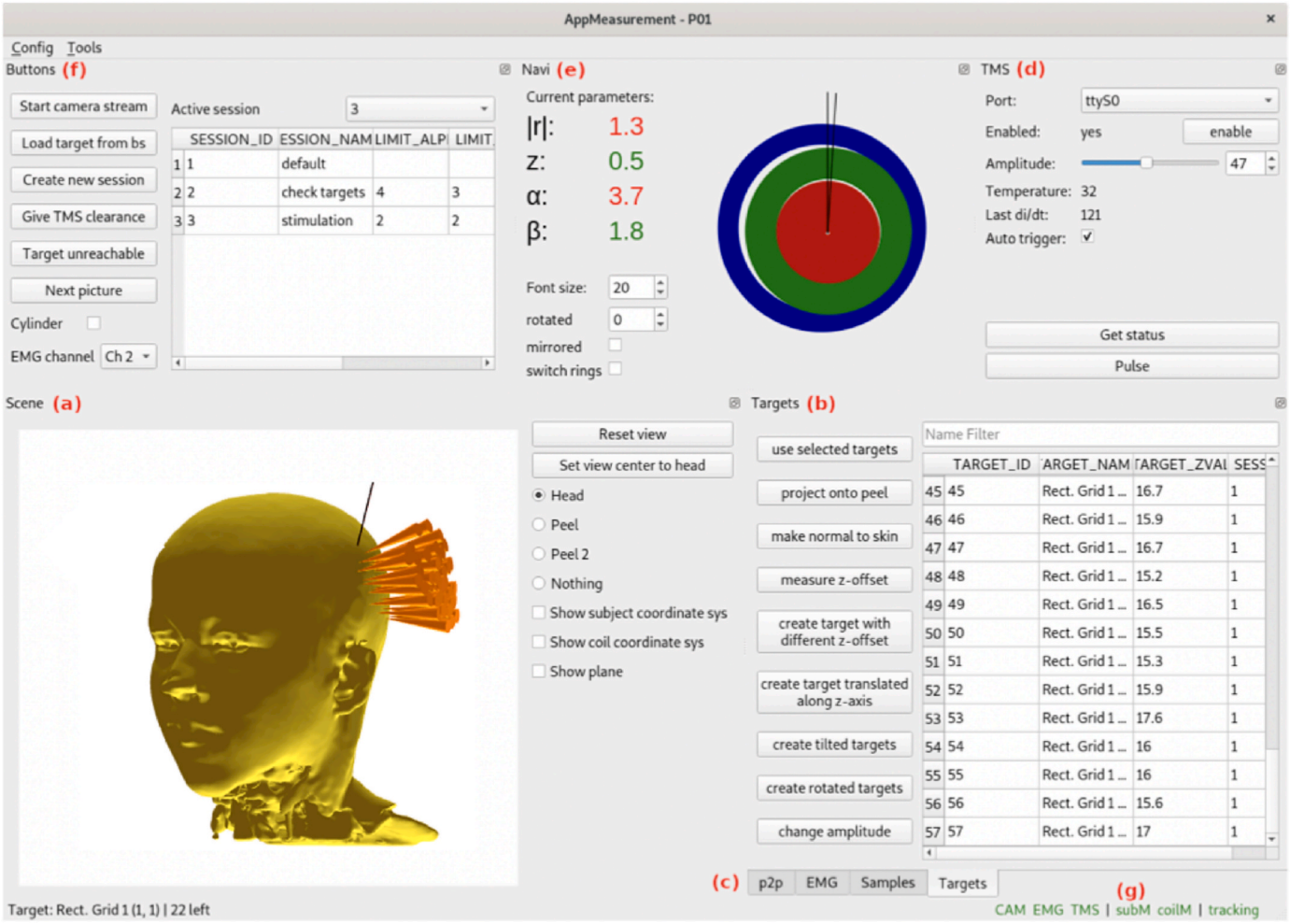


Fig. 2. Screenshot of the Precision Stimulation Software used for stimulation during the object naming paradigm with a) the 3D view of the scene with the selected targets in orange, b) a list of available targets, c) selection of dock windows, d) control keys for communication to TMS device, e) pre-set parameters for coil position and orientation with composition of circles to guide coil navigation, f) buttons for setting up and starting a new session, and g) indication of established communication to peripheral devices. (For interpretation of the references to colour in this figure legend, the reader is referred to the Web version of this article.)



Fig. 3. Screenshot of TMS language mapping procedure recording that was used for offline analysis. In the upper right corner of the screen a lighting bolt appears at the onset of the TMS bursts. On the left bottom corner the intended name for the object on the screen appears next to the trial number. The background of the video shows both the subject from their right side and the presentation screen. The foreground of the video in the right bottom corner shows the experimenter and the subject from their left side.

3. Results

All of the 23 subjects underwent fMRI measurements including resting-state and language task. Consequently, they all participated in a TMS language mapping session on the same day. Five subjects were excluded from the analysis as they did not exhibit any obvious naming

errors during the TMS language mapping procedure. Consequently, the results reported here are based on data from 18 out of 23 subjects initially recruited.

3.1. Functional language localizer

For all subjects, language fMRI resulted in increased activity in the inferior frontal lobe, anterior midline, the superior temporal lobe, anterior insula and inferior parietal lobules, $p < 0.05$ FWE-corrected. A group-map of the task activation of the contrast forward > backward is depicted in the Supplementary Fig. 1. For each individual, the peak within the STG was derived by taking the coordinates of the peak value within the STG from the forward > backward contrast.

3.2. TMS language mapping

All of the subjects completed the TMS language mapping session at 100% of their individually determined rMT. None of the subjects reported discomfort during or after the stimulation session. Each subject received 120 TMS bursts of 5 pulses at 10 Hz on the target grid placed around their functionally defined language peak. During stimulation 107 naming errors were observed. The most commonly observed naming errors were anomia (53.27%), followed by speech arrest (28.97%), semantic paraphasias (12.15%) and phonological paraphasia (5.61%). Absolute numbers of naming errors per category for each subject are reported in Supplementary Table 1.

The distributions of the spatially normalized mean E-fields for each error type are depicted in Fig. 4. The standard deviation of E-field distributions for each naming error category are depicted in Supplementary Fig. 2. The mean E-field for phonological paraphasia was spread across the posterior superior temporal gyrus, parts of the middle temporal gyrus and the angular gyrus, with the peak centered around MNI: −68, −46, 6. The E-field for semantic paraphasia covered the superior temporal gyrus, middle temporal gyrus and the angular gyrus as well. The peak was centered around MNI: −65, −50, 22. The difference between the mean E-fields for phonological versus semantic paraphasia is seen in the distribution of higher E-field values across the superior temporal gyrus. The mean E-field distributions causing speech arrest and anomia involved the superior temporal and posterior medial temporal gyrus. The peak values were located adjacent to each other. The peak for speech arrest was centered around MNI: −67, −50, 12 and for anomia around MNI: −65, 50, 21.

3.3. Resting-state

Group-level connectivity maps were calculated for the four different seeds derived from the mean effective E-fields for each naming error (i.e., anomia, speech arrest, semantic paraphasia and phonological paraphasia). In Fig. 5 the TMS language mapping results, including the E-field calculations and the resting-state networks for each language error,

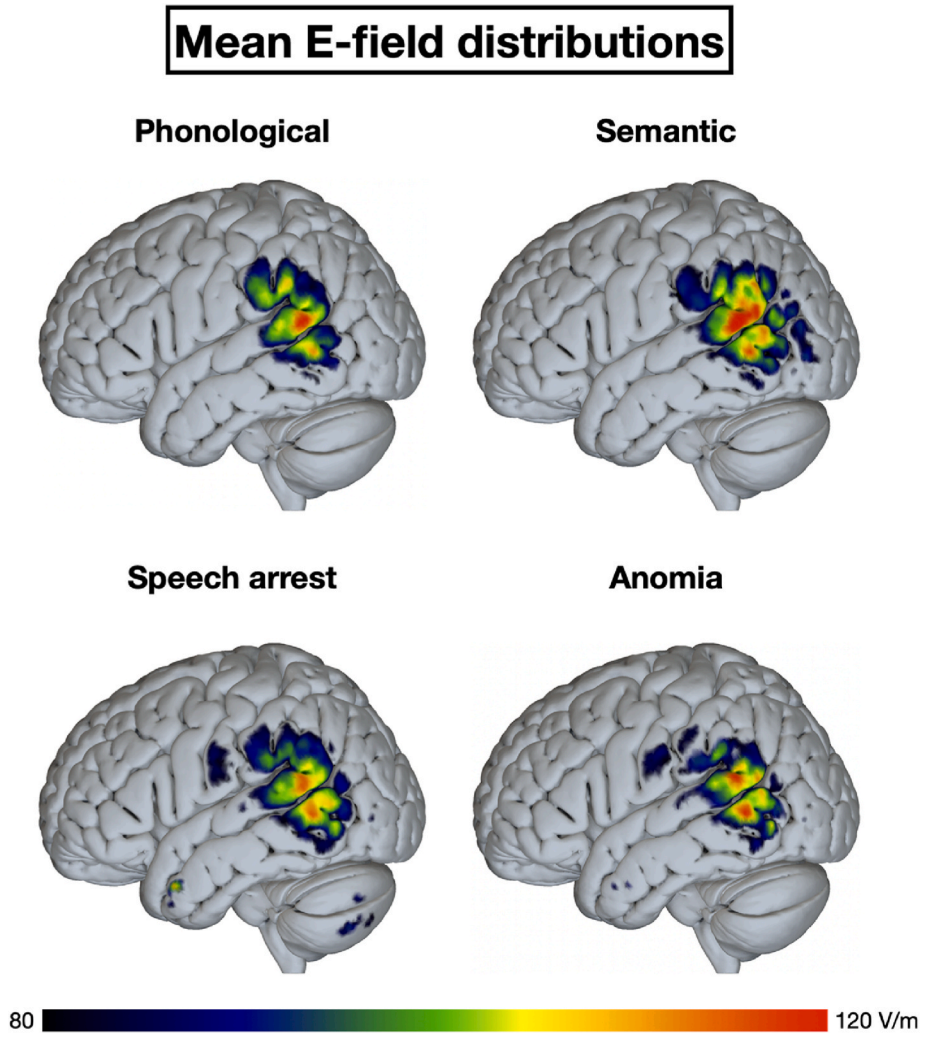


Fig. 4. Mean E-field distributions of the spatially normalized E-fields for each naming error type. Peaks were located at MNI: −68, −46, −6 for phonological paraphasia, at MNI: −65, −50, 22 for semantic paraphasia, at MNI: −67, −50, 12 for speech arrest and at MNI: −65, 50, 21 for anomia.

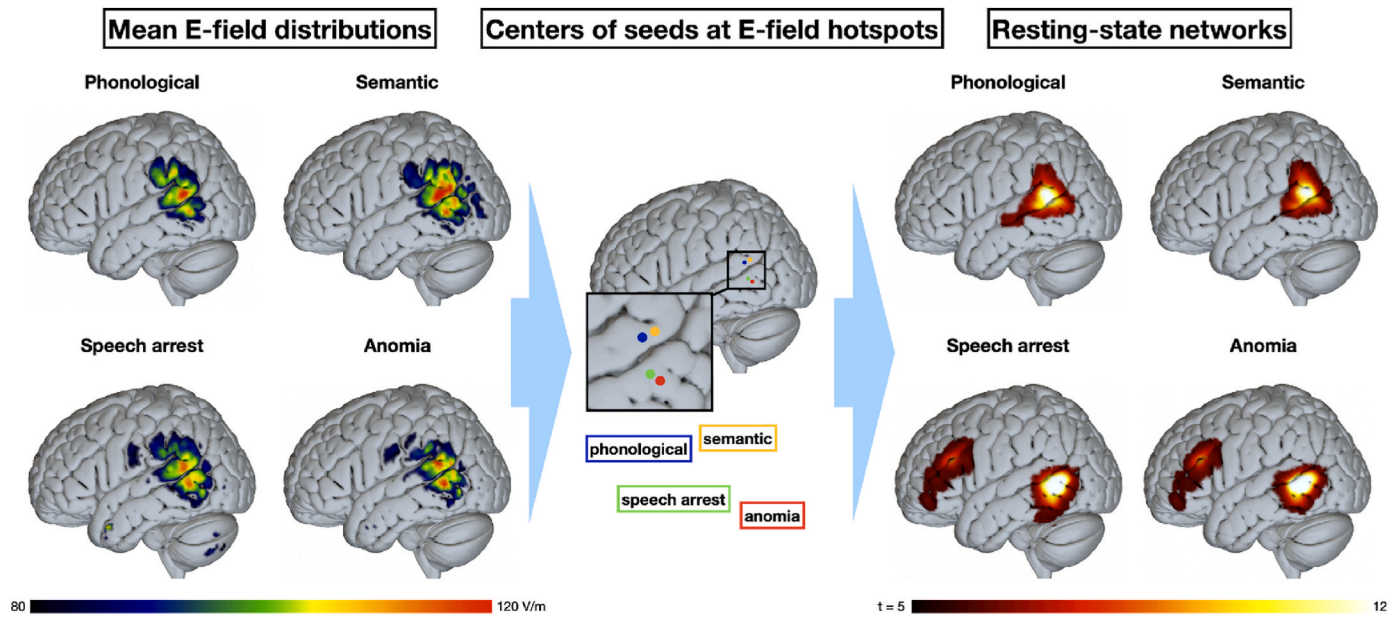


Fig. 5. The peaks of each mean E-field distribution were used as centers to create 6 mm spherical seeds. From these seeds the resting-state networks were calculated for each language error. The resting-state network for phonological and semantic paraphasia shows strong positive correlation from the seed area to areas surrounding the posterior STG, including the angular gyrus and the middle STG ($p < 0.05$, FWE-corrected). The resting-state connectivity for speech arrest and anomia show positive correlation from the seed area to the posterior middle temporal gyrus and the inferior frontal gyrus.

are summarized. Statistically significant differences were found for the contrast between a) RSNs of semantic and phonological error versus b) RSNs of anomia and speech arrest ($t = 4.55$, FWE $p < 0.05$). The latter seeds showed more positive connectivity to regions in the frontal lobe including the inferior frontal gyrus, middle frontal gyrus, dorsolateral prefrontal gyrus, and the posterior medial and inferior temporal gyrus. There were no statistically significant differences found between the brain areas included in the resting-state connectivity network for speech arrest and anomia. In the same manner, no statistical differences were found between the resting-state connectivity of the phonological and semantic paraphasia seeds. The anomia and speech arrest seeds largely overlapped as did the phonological and semantic seeds due to the proximity of the E-field peaks and therefore centers of the seed.

4. Discussion

This study investigated the dissociation of subregions of the posterior temporal gyrus based on their selective recruitment in language production. In a group of healthy subjects, short bursts of rTMS were applied to nodes of a target grid centered around a functionally defined language peak within the STG during the performance of a picture naming paradigm. The speech disruptions as a consequence of stimulation were recorded and categorized as anomia, speech arrest, phonological paraphasia or semantic paraphasia by three experienced raters. Through a unique combination of high precision stimulation software and E-field modeling, we mapped the different naming errors to reveal a dissociation of language functions within the temporal gyrus. Finally, we validated the functional engagement of these areas by means of resting-state fMRI in order to reveal specific functional connectivity patterns of the targets.

4.1. Language localizer

The results from our language localizer showed involvement of the typical language areas in the left hemisphere when comparing forward versus backward speech, including the inferior frontal lobe, the posterior temporal lobe, the angular gyrus and the occipitotemporal cortex. These results are in accordance with models for auditory sentence comprehension. For instance, one of the most prevailing models for sentence comprehension is the dorsal and ventral stream model [47–51]. According to this dual-stream model a specific ventral stream interfacing sounds with semantic representations, involves the left anterior inferior frontal gyrus, the left anterior superior temporal gyrus, the left middle temporal gyrus and the left occipitotemporal cortex. In a large review of neuroimaging studies on heard speech, spoken language and reading [52], proposes an anatomical model comprising a brain map of auditory semantic areas. In this model, the auditory semantic processing is thought to activate left-lateralized areas. The anterior and posterior regions of the superior temporal lobe are thought to be specialized for semantic composition and phonological perception, respectively. Neural activations for spoken sentences normally extend anteriorly to the temporal lobe. The inferior frontal areas are thought to subserve the selection of task-related semantic attributes, regarding the current study that entails understanding if the semantic attribute of the target word fits the sentence. The integration of these semantic features is thought to recruit the angular gyri. The activation pattern found in the group analysis of the language localizer data in the current study is consistent with the results of this review.

4.2. TMS language mapping

Concerning language mapping, TMS can be used to evoke so-called virtual lesions to interfere with language processing [53]. Several studies already showed the application of TMS over temporal regions during language production tasks [13–23]. However, the technical limitations of the previous studies did not allow for precise dissociation of language functions. Causal function to cortex mapping can be advanced by introducing E-field modeling [54]. used electric field neuronavigation during stimulation to evaluate systematic adjustments of the stimulation protocol. The online electric field navigation approximates the actual induced E-field in the cortex and gives direction in deciding on stimulation dose and stimulation target [55]. However, it does not take into consideration the conductivity properties of the underlying tissue types. An offline approach which allows for simulation of realistic calculations of the electric field induced by TMS is SimNIBS (SimNIBS 3.2.6 [45]). A large advantage of SimNIBS is the clear link

between the induced electric fields and the physiological stimulation effects. Using this offline E-field modeling approach, we were able in the current study to distinguish posterior temporal regions underlying different naming errors. The results clearly show an anatomical-functional relational division between effective E-field distributions for phonological and semantic paraphasia on the one hand, and anomia and speech arrest on the other hand.

4.3. Phonological and semantic paraphasia

The effective E-field distribution maps for phonological and semantic paraphasia showed a large spatial overlap which was most prominent in the posterior STG. These results are largely in line with the findings from an extensive meta-analysis of neuroimaging studies of the functional organization of the language network focused on the division and similarity between semantics and phonology [56]. The results from this meta-analysis showed that semantic and phonological processing consistently recruited many overlapping regions, namely the posterior temporal gyrus and the supramarginal gyrus (SMG). However for semantic processing more activation was found in the middle temporal gyrus and the angular gyrus. Whereas for phonological processing, activations were predominantly found in the posterior STG and the SMG. In the current study, the most prominent differences between the effective E-fields for semantic and phonological paraphasia can be seen in the extension of the distribution for semantic paraphasia into the angular and supramarginal gyrus. While our results diverge in some ways from the results of [56], they are largely in concordance with previous navigated TMS language mapping studies. For instance Ref. [14], showed that the most prominent regions for semantic and phonological paraphasia were the posterior medial frontal gyrus and the anterior SMG. They included a category of performance errors which also entailed slurred speech and phonological errors. For this category the most important area was the anterior STG. This is in line with the peak of the effective phonological E-field distribution found in the current study being anterior to the peak of the effective semantic E-field distribution. In addition [16], performed TMS language mapping in a small sample of healthy subjects and found that phonological and semantic errors were more likely to occur when stimulating the SMG region. Using the same methodology [18], found that stimulation of the medial and posterior STG as well as the SMG, resulted in phonological paraphasia. Whereas stimulation of the posterior MTG and the SMG resulted in most semantic paraphasia. Importantly, stimulation of the SMG resulted in semantic paraphasia more often compared to phonological paraphasia.

Further, the shape and extent of effective E-field distributions resulting in semantic and phonological paraphasia, are largely in line with the topographical gradients of semantic and phonological processing found by Ref. [57]. The authors analyzed naming errors induced by left temporal cortical stimulation in epilepsy surgery patients. The distribution of stimulation sites causing semantic errors was widely spread along the temporal lobe, with a large concentration in the medial temporal gyrus. Whereas the distribution of stimulation sites leading to phonological errors was rather focal and concentrated around the superior temporal gyrus.

Taken together with the results of the current study as well as from previous TMS language mapping studies, there seems to be a gradient according to which the angular gyrus and the SMG are involved in semantic processing and the STG in phonological processing. Causes of semantic and phonological paraphasia in posterior temporal and anterior parietal regions in a virtual-lesion model via TMS stimulation seem to fit the hypothesis of semantic activation and lexical selection in the posterior region [58,59].

4.4. Anomia and speech arrest

The distribution of average effective E-fields resulting in speech arrests and anomia covered largely the same areas, namely the posterior medial temporal gyrus and the posterior superior temporal gyrus. The effects of TMS over the STG leading to no-response and performance errors (i.e. anomia and speech arrest) have been previously shown by Ref. [14]. In a similar manner [16], showed non-response errors mainly following stimulation of the STG and SMG. Following the same method [54], found non-response errors following stimulation of the angular gyrus and the posterior superior temporal gyrus. The results found in the current study differ from these previous language TMS mapping studies in that a large proportion of the non-response errors in the current study were caused by stimulation of the posterior medial temporal gyrus. However [19], found anomia and speech arrest errors in some of their subjects when stimulating the middle temporal gyrus. In addition, no response errors as a result of middle temporal gyrus stimulation were also found by Ref. [57]. Moreover, involvement of both the STG and MTG in stages leading to word production have been reported in non-invasive studies as well [8,60,61]. The process of language production involves several stages, including the planning of what to say, the selection and organization of the words, phonemes and grammatical structures that will be used, and the production of the verbal output [62]. Inferring from past studies on the relation between function and anatomical location, naming errors following stimulation of these cortical regions could be due to restricted semantic and/or phonological processing, by blocking access to, and the retrieval of, semantic and phonological representation [63].

4.5. Resting-state

TMS effects are thought to affect not only the area directly beneath the coil, but to influence remote and interconnected areas [27–30]. An additional aspect in our study aimed to explain the different effective E-field distributions found for semantic/phonological paraphasia and anomia/speech arrest and the consequence on whole-brain networks. In order to validate the functional selectivity of the resulting maps, we performed resting-state network analysis for each peak of the E-field derived maps.

The functional connectivity for the cortical regions involved in naming errors related to phonological and semantic processing were largely overlapping. For both error types, the regions functionally connected to the respective peaks of the effective E-fields were located within the temporal lobe. However, the resting-state network for phonological processing extended further to the anterior parts of the STG and MTG. These results are in line with anatomical models of language processing that hold that phonological representation and processing may involve an extension from the posterior STG to more anterior regions in the STG [64]. The results concerning semantic errors are in line with the previously discussed studies suggesting altogether that more posterior and superior areas of the temporal gyrus and the temporal-parietal junction (i.e. SMG and angular gyrus) are involved in semantic processing and the STG and the MTG in phonological processing. On the other hand, the resting-state networks of anomia and speech arrest show large overlap in functionally connected regions in the IFG, suggesting that stimulation of these areas in the posterior temporal lobes engage a larger network for speech production [65]. Taken together, the resting-state results for phonological and semantic peaks are hinting towards a more local network disruption effect within the temporal lobe, while anomia and speech arrest underlie the disruption of a larger network including the IFG. This might suggest that STG stimulation results in more subtle retrieval errors by interrupting local processes [52,66], while MTG stimulation interferes with the whole ventral pathway of lexico-semantic processing, which results in more severe impairments in task-performance [63].

4.6. Limitations

A potential limitation of the current study is the relatively small

number of effective trials. TMS over the STG resulted in naming errors in 107 trials spread across 18 subjects and four error categories. One potential consequence may be that the results presented in this manuscript, particularly those related to phonological and semantic processing, may not accurately represent or generalize to all individuals. It is crucial to acknowledge that there can be significant spatial subject-to-subject variability in effective E-fields as revealed by the standard deviation maps (Supplementary Fig. 2), and thus caution must be exercised when interpreting these findings. The observed results should be considered within the context of individual differences, and future studies should further investigate this variability to obtain a more comprehensive understanding of the generalizability of the results. However, previous research shows that TMS language mapping typically has a higher negative predictive value as validated with DCS [15,17,19], which means that even when the stimulation does not elicit a language-related response, it still provides significant information for identifying areas in the brain that are not involved in language processing. In other words, the ineffective TMS sites provide critical information in determining language-negative regions. There are several options to increase the absolute number of effective trials in future studies. For instance, the number of stimulations per target could be increased during the language mapping paradigm or the paradigm could be repeated several times. However, it's important to consider the trade-off between subject compliance and sample size. In a recent publication a method was proposed to localize cortical muscle representation on an individual subject level by linking the induced E-field and the MEP [24]. It was suggested that obtaining robust cortical maps requires approximately 150 pulses from random coil positions and orientations. Although the current study does not focus on mapping the motor cortex representation, 120 bursts of 5 pulses per subject were applied at a predefined location, which, while not completely random, may be sufficient.

Another potential approach to improve the efficacy of TMS sites is to utilize a more specific fMRI localizer task. In our study, the stimulation grid was centered around the peak activation of a language localizer task involving language comprehension. Although this task produced strong language activation maps, it did not specifically target the language processes that were disrupted during the TMS language mapping paradigm (i.e. semantic processing, phonological processing or speech production). To address this limitation, future studies could consider incorporating more specific fMRI localizer tasks (e.g. an object naming paradigm), this could enhance the relevance and precision of TMS language mapping. For instance Ref. [67], employed a method to model the impact of TMS on spatial attention. Their approach involved first localizing attentional processes using an fMRI spatial attention task. Subsequently, TMS was administered during the same attention task, targeting the individually defined regions. The analysis of the results revealed contrasting patterns in BOLD-measured neuronal activity and TMS-evoked neuronal effects, highlighting an important distinction in how neural activity is related to paradigms and behavioral outcomes.

A limitation of the present study is the potential involvement of neighboring areas, which cannot be completely ruled out. The effectiveness of transcranial magnetic stimulation (TMS) in terms of spatial resolution is heavily influenced by individual cortical folding patterns [68]. The current study focuses on regions with pronounced cortical folding, i.e. the superior temporal gyrus (STG). Consequently, it becomes challenging to distinguish between adjacent regions. Achieving functional separation of neighboring regions with distinct depth profiles presents a particularly complex task [69]. However, adopting such an approach could yield valuable insights into the interplay and potential synergistic effects among different brain regions involved in phenomena like anomia. By investigating the simultaneous stimulation of multiple sites, we can potentially enhance our comprehension of the neural mechanisms that underlie language processes.

5. Conclusion

The combination of fMRI, TMS mapping and E-field modeling can disentangle the dissociation of language functions within the temporal gyrus. This highly advanced and precise mapping method can influence cortical mapping of cognitive functions considerably. Our results clearly show that using the combination of neuroimaging and stimulation, allows for delineating cortical areas underlying sub-functions of a cognitive domain, i.e. language production. In addition, we were able to show that these cortical areas are differentially connected to other parts of the language network. This supports the hypothesis of the behavioral specificity of the temporal gyrus in language production. Taken together, our study provides important insights on the functional neuroanatomy of language production and might help to increase the current understanding of specific language production difficulties.

CRediT authorship contribution statement

Maria Vasileiadi: Conceptualization, Writing – original draft, Formal analysis, Investigation, Visualization, Data curation, Funding acquisition. **Anna-Lisa Schuler:** Conceptualization, Writing – review & editing. **Michael Woletz:** Formal analysis, Writing – review & editing. **David Linhardt:** Visualization, Writing – review & editing. **Christian Windischberger:** Resources, Writing – review & editing. **Martin Tik:** Supervision, Conceptualization, Writing – review & editing.

Declaration of competing interest

We wish to confirm that there are no known conflicts of interest associated with this publication and there has been no significant financial support for this work that could have influenced its outcome.

We confirm that the manuscript has been read and approved by all named authors and that there are no other persons who satisfied the criteria for authorship but are not listed. We further confirm that the order of authors listed in the manuscript has been approved by all of us.

We confirm that we have given due consideration to the protection of intellectual property associated with this work and that there are no impediments to publication, including the timing of publication, with respect to intellectual property. In so doing we confirm that we have followed the regulations of our institutions concerning intellectual property.

We further confirm that any aspect of the work covered in this manuscript that has involved either experimental animals or human patients has been conducted with the ethical approval of all relevant bodies and that such approvals are acknowledged within the manuscript.

We understand that the Corresponding Author is the sole contact for the Editorial process (including Editorial Manager and direct communications with the office). He is responsible for communicating with the other authors about progress, submissions of revisions and final approval of proofs. We confirm that we have provided a current, correct email address which is accessible by the Corresponding Author and which has been configured to accept email from martin.tik@meduniwien.ac.at.

Acknowledgments

This research was supported by the Austrian Academy of Sciences (DOC).

Appendix A. Supplementary data

Supplementary data to this article can be found online at https://doi.org/10.1016/j.brs.2023.06.014.

References

[1] Caramazza A, Zurif EB. Dissociation of algorithmic and heuristic processes in language comprehension: evidence from aphasia. Brain Lang 1976;3:572–82. https://doi.org/10.1016/0093-934X(76)90048-1.

[2] Nicolosi L, Harryman E, Kresheck J. Terminology of communication disorders: speech-language-hearing. Lippincott Williams & Wilkins; 2004.

[3] Rutten G-J. Chapter 2 - Broca-Wernicke theories: a historical perspective. In: Hillis AE, Fridriksson J, editors. Handb. Clin. Neurol., 185. Elsevier; 2022. p. 25–34. https://doi.org/10.1016/B978-0-12-823384-9.00001-3.

[4] de Zubicaray GI, Piai V. Investigating the spatial and temporal components of speech production. In: de Zubicaray GI, Schiller NO, editors. Oxf. Handb. Neurolinguistics. Oxford University Press; 2019. p. 471–97. https://doi.org/10.1093/oxfordhb/9780190672027.013.19.

[5] Binder JR. The Wernicke area: modern evidence and a reinterpretation. Neurology 2015;85:2170–5. https://doi.org/10.1212/WNL.0000000000002219.

[6] Binder JR, Tong J, Pillay SB, Conant LL, Humphries CJ, Raghavan M, et al. Temporal lobe regions essential for preserved picture naming after left temporal epilepsy surgery. Epilepsia 2020;61:1939–48. https://doi.org/10.1111/epi.16643.

[7] Gernsbacher MA, Kaschak MP. Neuroimaging studies of language production and comprehension. Annu Rev Psychol 2003;54:91–114. https://doi.org/10.1146/annurev.psych.54.101601.145128.

[8] Indefrey P. The spatial and temporal signatures of word production components: a critical update. Front Psychol 2011;2. https://doi.org/10.3389/fpsyg.2011.00255.

[9] Nasios G, Dardiotis E, Messinis L. From Broca and wernicke to the neuromodulation era: insights of brain language networks for neurorehabilitation. Behav Neurol 2019;2019:1–10. https://doi.org/10.1155/2019/9894571.

[10] Stark BC, Basilakos A, Hickok G, Rorden C, Bonilha L, Fridriksson J. Neural organization of speech production: a lesion-based study of error patterns in connected speech. Cortex 2019;117:228–46. https://doi.org/10.1016/j.cortex.2019.02.029.

[11] Sarubbo S, Tate M, De Benedictis A, Merler S, Moritz-Gasser S, Herbet G, et al. A normalized dataset of 1821 cortical and subcortical functional responses collected during direct electrical stimulation in patients undergoing awake brain surgery. Data Brief 2020;28:104892. https://doi.org/10.1016/j.dib.2019.104892.

[12] Sarubbo S, Tate M, De Benedictis A, Merler S, Moritz-Gasser S, Herbet G, et al. Mapping critical cortical hubs and white matter pathways by direct electrical stimulation: an original functional atlas of the human brain. Neuroimage 2020;205:116237. https://doi.org/10.1016/j.neuroimage.2019.116237.

[13] Klaus J, Hartwigsen G. Dissociating semantic and phonological contributions of the left inferior frontal gyrus to language production. Hum Brain Mapp 2019;40:3279–87. https://doi.org/10.1002/hbm.24597.

[14] Krieg SM, Sollmann N, Tanigawa N, Foerschler A, Meyer B, Ringel F. Cortical distribution of speech and language errors investigated by visual object naming and navigated transcranial magnetic stimulation. Brain Struct Funct 2016;221:2259–86. https://doi.org/10.1007/s00429-015-1042-7.

[15] Krieg SM, Tarapore PE, Picht T, Tanigawa N, Houde J, Sollmann N, et al. Optimal timing of pulse onset for language mapping with navigated repetitive transcranial magnetic stimulation. Neuroimage 2014;100:219–36. https://doi.org/10.1016/j.neuroimage.2014.06.016.

[16] Lioumis P, Zhdanov A, Mäkelä N, Lehtinen H, Wilenius J, Neuvonen T, et al. A novel approach for documenting naming errors induced by navigated transcranial magnetic stimulation. J Neurosci Methods 2012;204:349–54. https://doi.org/10.1016/j.jneumeth.2011.11.003.

[17] Picht T, Krieg SM, Sollmann N, Rösler J, Niraula B, Neuvonen T, et al. A comparison of language mapping by preoperative navigated transcranial magnetic stimulation and direct cortical stimulation during awake surgery. Neurosurgery 2013;72:808–19. https://doi.org/10.1227/NEU.0b013e3182889e01.

[18] Rösler J, Niraula B, Strack V, Zdunczyk A, Schilt S, Savolainen P, et al. Language mapping in healthy volunteers and brain tumor patients with a novel navigated TMS system: evidence of tumor-induced plasticity. Clin Neurophysiol 2014;125:526–36. https://doi.org/10.1016/j.clinph.2013.08.015.

[19] Tarapore PE, Findlay AM, Honma SM, Mizuiri D, Houde JF, Berger MS, et al. Language mapping with navigated repetitive TMS: proof of technique and validation. Neuroimage 2013;82:260–72. https://doi.org/10.1016/j.neuroimage.2013.05.018.

[20] Tarapore PE, Picht T, Bulubas L, Shin Y, Kulchytska N, Meyer B, et al. Safety and tolerability of navigated TMS for preoperative mapping in neurosurgical patients. Clin Neurophysiol 2016;127:1895–900. https://doi.org/10.1016/j.clinph.2015.11.042.

[21] Töpper R, Mottaghy FM, Brügmann M, Noth J, Huber W. Facilitation of picture naming by focal transcranial magnetic stimulation of Wernicke's area. Exp Brain Res 1998;121:371–8. https://doi.org/10.1007/s002210050471.

[22] Raffa G, Bährend I, Schneider H, Faust K, Germanò A, Vajkoczy P, et al. A novel technique for region and linguistic specific nTMS-based DTI fiber tracking of language pathways in brain tumor patients. Front Neurosci 2016;10:552.

[23] Sollmann N, Fuss-Ruppenthal S, Zimmer C, Meyer B, Krieg SM. Investigating stimulation protocols for language mapping by repetitive navigated transcranial magnetic stimulation. Front Behav Neurosci 2018;12.

[24] Numssen O, Zier A-L, Thielscher A, Hartwigsen G, Knösche TR, Weise K. Efficient high-resolution TMS mapping of the human motor cortex by nonlinear regression. Neuroimage 2021;245:118654.

[25] Weise K, Numssen O, Thielscher A, Hartwigsen G, Knösche TR. A novel approach to localize cortical TMS effects. Neuroimage 2020;209:116486.

[26] Weise K, Numssen O, Kalloch B, Zier AL, Thielscher A, Haueisen J, et al. Precise motor mapping with transcranial magnetic stimulation. Nat Protoc 2022:1–26.

[27] Fox MD, Halko MA, Eldaief MC, Pascual-Leone A. Measuring and manipulating brain connectivity with resting state functional connectivity magnetic resonance imaging (fcMRI) and transcranial magnetic stimulation (TMS). Neuroimage 2012;62:2232–43. https://doi.org/10.1016/j.neuroimage.2012.03.035.

[28] Siddiqi SH, Kording KP, Parvizi J, Fox MD. Causal mapping of human brain function. Nat Rev Neurosci 2022;23:361–75. https://doi.org/10.1038/s41583-022-00583-8.

[29] Tik M, Woletz M, Schuler A, Vasileiadi M, Cash RFH, Zalesky A, et al. Acute TMS/fMRI response explains offline TMS network effects – an interleaved TMS-fMRI study. Neuroimage 2022:119833. https://doi.org/10.1016/j.neuroimage.2022.119833.

[30] Vink JJT, Mandija S, Petrov PI, van den Berg CAT, Sommer IEC, Neggers SFW. A novel concurrent TMS-fMRI method to reveal propagation patterns of prefrontal magnetic brain stimulation. Hum Brain Mapp 2018;39:4580–92. https://doi.org/10.1002/hbm.24307.

[31] Tik M, Hoffmann A, Sladky R, Tomova L, Hummer A, Navarro de Lara L, et al. Towards understanding rTMS mechanism of action: stimulation of the DLPFC causes network-specific increase in functional connectivity. Neuroimage 2017;162:289–96. https://doi.org/10.1016/j.neuroimage.2017.09.022.

[32] Tik M, Woletz M, Schuler AL, Vasileiadi M, Cash RFH, Zalesky A, et al. Acute TMS/fMRI response explains offline TMS network effects–An interleaved TMS-fMRI study. NeuroImage 2023;267:119833.

[33] Tik M, Hoffmann A, Sladky R, Tomova L, Hummer A, de Lara. Towards understanding rTMS mechanism of action: stimulation of the DLPFC causes network-specific increase in functional connectivity. Neuroimage 2017;162:289–296.Chicago.

[34] Cash RF, Weigand A, Zalesky A, Siddiqi SH, Downar J, Fitzgerald PB, et al. Using brain imaging to improve spatial targeting of transcranial magnetic stimulation for depression. Biol psychiatr 2021;90(10):689–700.

[35] Castrillon G, Sollmann N, Kurcyus K, Razi A, Krieg SM, Riedl V. The physiological effects of noninvasive brain stimulation fundamentally differ across the human cortex. Sci Adv 2020;6:eaay2739. https://doi.org/10.1126/sciadv.aay2739.

[36] Schuler A-L, Tik M, Sladky R, Luft CDB, Hoffmann A, Woletz M, et al. Modulations in resting state networks of subcortical structures linked to creativity. Neuroimage 2019;195:311–9.

[37] Krieg SM, Lioumis P, Mäkelä JP, Wilenius J, Karhu J, Hannula H, et al. Protocol for motor and language mapping by navigated TMS in patients and healthy volunteers; workshop report. Acta Neurochir 2017;159:1187–95. https://doi.org/10.1007/s00701-017-3187-z.

[38] Berl MM, Mayo J, Parks EN, Rosenberger LR, VanMeter J, Ratner NB, et al. Regional differences in the developmental trajectory of lateralization of the language network: developmental Trajectories of Lateralization of Language. Hum Brain Mapp 2014;35:270–84. https://doi.org/10.1002/hbm.22179.

[39] Moeller S, Yacoub E, Olman CA, Auerbach E, Strupp J, Harel N, et al. Multiband multislice GE-EPI at 7 tesla, with 16-fold acceleration using partial parallel imaging with application to high spatial and temporal whole-brain fMRI. Magn Reson Med 2010;63:1144–53. https://doi.org/10.1002/mrm.22361.

[40] Vasileiadi M, Woletz M, Linhardt D, Grosshagauer S, Tik M, Windischberger C. Improved brain stimulation targeting by optimising image acquisition parameters. NeuroImage 2023;276:12017. https://doi.org/10.1016/j.neuroimage.2023.120175.

[41] Sladky R, Friston KJ, Tröstl J, Cunnington R, Moser E, Windischberger C. Slice-timing effects and their correction in functional MRI. Neuroimage 2011;58:588–94. https://doi.org/10.1016/j.neuroimage.2011.06.078.

[42] Avants BB, Tustison NJ, Song G, Cook PA, Klein A, Gee JC. A reproducible evaluation of ANTs similarity metric performance in brain image registration. Neuroimage 2011;54:2033–44. https://doi.org/10.1016/j.neuroimage.2010.09.025.

[43] Koivisto M, Revonsuo A. Event-related brain potential correlates of visual awareness. Neurosci Biobehav Rev 2010;34:922–34. https://doi.org/10.1016/j.neubiorev.2009.12.002.

[44] Szekely A, Damico S, Devescovi A, Federmeier K, Herron D, Iyer G, et al. Timed action and object naming. Cortex 2005;41:7–25. https://doi.org/10.1016/S0010-9452(08)70174-6.

[45] Thielscher A, Antunes A, Saturnino GB. Field modeling for transcranial magnetic stimulation: a useful tool to understand the physiological effects of TMS? 2015 37th. Annu. Int. Conf. IEEE Eng. Med. Biol. Soc. EMBC 2015:222–5. https://doi.org/10.1109/EMBC.2015.7318340.

[46] Drakaki M, Mathiesen C, Siebner HR, Madsen K, Thielscher A. Database of 25 validated coil models for electric field simulations for TMS. Brain Stimul 2022;15:697–706. https://doi.org/10.1016/j.brs.2022.04.017.

[47] Friederici AD. The brain basis of language processing: from structure to function. Physiol Rev 2011;91.

[48] Friederici AD. The cortical language circuit: from auditory perception to sentence comprehension, 16; 2012.

[49] Hickok G, Poeppel D. Towards a functional neuroanatomy of speech perception. Trends Cognit Sci 2000;4:131–8. https://doi.org/10.1016/S1364-6613(00)01463-7.

[50] Hickok G, Poeppel D. Dorsal and ventral streams: a framework for understanding aspects of the functional anatomy of language 2004.

[51] Hickok G, Poeppel D. The cortical organization of speech processing. Nat Rev Neurosci 2007;8:393–402. https://doi.org/10.1038/nrn2113.

[52] Price CJ. A review and synthesis of the first 20years of PET and fMRI studies of heard speech, spoken language and reading. Neuroimage 2012;62:816–47. https://doi.org/10.1016/j.neuroimage.2012.04.062.
[53] Walsh V, Cowey A. Transcranial magnetic stimulation and cognitive neuroscience. Nat Rev Neurosci 2000;1:73–80. https://doi.org/10.1038/35036239.
[54] Sollmann N, Fuss-Ruppenthal S, Zimmer C, Meyer B, Krieg SM. Investigating stimulation protocols for language mapping by repetitive navigated transcranial magnetic stimulation. Front Behav Neurosci 2018;12:197.
[55] Ruohonen J, Karhu J. Navigated transcranial magnetic stimulation. Neurophysiol Clin Neurophysiol 2010;40:7–17. https://doi.org/10.1016/j.neucli.2010.01.006.
[56] Hodgson VJ, Lambon Ralph MA, Jackson RL. Multiple dimensions underlying the functional organization of the language network. Neuroimage 2021;241:118444. https://doi.org/10.1016/j.neuroimage.2021.118444.
[57] Miozzo M, Williams AC, McKhann II GM, Hamberger MJ. Topographical gradients of semantics and phonology revealed by temporal lobe stimulation. Hum Brain Mapp 2017;38:688–703. https://doi.org/10.1002/hbm.23409.
[58] Corina DP, Loudermilk BC, Detwiler L, Martin RF, Brinkley JF, Ojemann G. Analysis of naming errors during cortical stimulation mapping: implications for models of language representation. Brain Lang 2010;115:101–12. https://doi.org/10.1016/j.bandl.2010.04.001.
[59] Xiang H-D, Fonteijn HM, Norris DG, Hagoort P. Topographical functional connectivity pattern in the perisylvian language networks. Cerebr Cortex 2010;20:549–60. https://doi.org/10.1093/cercor/bhp119.
[60] Salmelin R, Hari R, Lounasmaa OV, Sams M. Dynamics of brain activation during picture naming. Nature 1994;368:463–5. https://doi.org/10.1038/368463a0.
[61] Vihla M, Laine M, Salmelin R. Cortical dynamics of visual/semantic vs. phonological analysis in picture confrontation. Neuroimage 2006;33:732–8. https://doi.org/10.1016/j.neuroimage.2006.06.040.
[62] Indefrey P, Levelt WJM. The spatial and temporal signatures of word production components. Cognition 2004;92:101–44. https://doi.org/10.1016/j.cognition.2002.06.001.
[63] Friederici AD, Gierhan SM. The language network. Curr Opin Neurobiol 2013;23:250–4.
[64] Levy O, Kenett YN, Oxenberg O, Castro N, De Deyne S, Vitevitch MS, et al. Unveiling the nature of interaction between semantics and phonology in lexical access based on multilayer networks. Sci Rep 2021;11:14479. https://doi.org/10.1038/s41598-021-93925-y.
[65] Silbert LJ, Honey CJ, Simony E, Poeppel D, Hasson U. Coupled neural systems underlie the production and comprehension of naturalistic narrative speech. Proc Natl Acad Sci USA 2014;111. https://doi.org/10.1073/pnas.1323812111.
[66] Price CJ. The anatomy of language: a review of 100 fMRI studies published in 2009. Ann N Y Acad Sci 2010;1191:62–88.
[67] Jing Y, Numssen O, Weise K, Kalloch B, Haueisen J, Hartwigsen G, et al. Modeling the effects of transcranial magnetic stimulation on spatial attention. Neuroscience 2023. https://doi.org/10.1101/2023.01.11.523548.
[68] Numssen O, van der Burght CL, Hartwigsen G. Revisiting the focality of non-invasive brain stimulation – implications for studies of human cognition. Neurosci Biobehav Rev 2023;149:105154. https://doi.org/10.1016/j.neubiorev.2023.105154.
[69] van der Burght CL, Numssen O, Schlaak B, Goucha T, Hartwigsen G. Differential contributions of inferior frontal gyrus subregions to sentence processing guided by intonation. Hum Brain Mapp 2023;44:585–98. https://doi.org/10.1002/hbm.26086.